Exact measurement of flat surface profiles by object shifts in a phase-conjugate Fizeau interferometer

Osami Sasaki, MEMBER SPIE
Yuuichi Takebayashi, MEMBER SPIE
Niigata University
Faculty of Engineering
8050 Ikarashi 2
Niigata-shi 950-21, Japan

Xiangzhao Wang
Niigata University
Graduate School of Science and Technology
8050 Ikarashi 2
Niigata-shi 950-21, Japan

Takamasa Suzuki, MEMBER SPIE
Niigata University
Faculty of Engineering
8050 Ikarashi 2
Niigata-shi 950-21, Japan

Abstract. We propose a method of exact measurement of flat surface profiles in a phase-conjugate Fizeau interferometer. Aberration of lenses causes an undesirable phase distribution in the interference signal of the phase-conjugate Fizeau interferometer. To eliminate this phase distribution, we shift the object in two directions orthogonal to each other and we get difference values of the surface profile of the object. Additional displacements of the object surface involved in the shifts lead to some small errors in the difference values. We estimate an exact surface profile by solving the difference equations. Characteristics of the method are made clear through computer simulations and measurements of a 40-mm-diam flat mirror.

Subject terms: flatness testing; interferometers; phase conjugation.

Optical Engineering 34(10), 2957–2963 (October 1995).

1 Introduction

When we make absolute measurement of an optical flat with a Fizeau interferometer, we use the three-flat method in which two flats are combined among three flats to provide an object surface and a reference surface.[1] Because Fizeau interferometers have a common path for the object and reference waves, aberrations of lenses and roughness of optical elements do not cause any undesirable phase distribution in an interference signal. The three-flat method is used to eliminate flatness deviation of the reference surface. This method has been developed into the rotation method[2–4] and the rotation shift method.[5] In the rotation method, three basic combinations and one rotational combination for the three flats are used to make absolute measurement on the entire surface of an object. In the rotation shift method, a parallel shift of a flat is incorporated in a basic combination, which is suitable to image detectors of a square grid structure.[5,6]

When we use a phase-conjugate Fizeau interferometer[7] in which the reference wave is a phase-conjugate wave of the object wave, aberrations of lenses and roughness of optical elements cause an undesirable phase distribution in an interference signal. To make exact measurement, we must consider a method different from the three-flat method. We propose a method of exact measurement of flat surface profile in the phase-conjugate Fizeau interferometer. In the method the object is shifted in two directions orthogonal to each other by the intervals of measuring points. These shifts provide difference values of the surface profile of an object assuming that the shifts do not change the undesirable phase distribution. This assumption is valid for optical flats whose variations of the surface profiles are so slow that the shifts of the object almost do not change the propagation direction of the light reflected by the object. In practice the shifts of the object involve additional displacements of the object surface. In order to eliminate effects of the displacement, we calculate the tilt and the average height of the raw detected phase distribution and subtract them from the raw detected phase distribution. This processing changes slightly a mathematical reference plane that is defined before the shifts and produces very small errors in the difference values of the surface profile of the object. This is why the measurement is not absolute. We obtain an exact surface profile by solving the difference equations. As a method of solving the equations, we use the conjugate gradient method to make the difference values of an estimated surface profile equal to the measured difference values.

In Sec. 2 we review a phase-conjugate interferometer, and in Sec. 3 we propose a method of exact measurement. Section 4 presents computer simulations to examine the effects of noise contained in the difference values and the effects of error in the distance of the shifts. In Sec. 5 experimental results of the exact measurement of a flat mirror are presented, and in Sec. 6 we discuss the effects of the small

Paper 26114 received Nov. 24, 1994; revised manuscript received Mar. 20, 1995; accepted for publication Mar. 20, 1995.

error contained in the difference values to show clearly the usefulness of the method.

2 Phase-Conjugate Fizeau Interferometer

To carry out exact measurements of optical flats, we use a phase-conjugate Fizeau interferometer that has already been reported in Ref. 7. Figure 1 shows a sinusoidal phase-modulating (SPM) Fizeau interferometer using a self-pumped phase-conjugate wave. By using this interferometer, we can measure surface profiles without being affected by the time-varying phase change of the object wave. A special feature of the interferometer is that it is completely free of the vibrations of objects. However, an interferometer using a phase-conjugate wave is sensitive to an undesirable phase distribution caused by aberrations of lenses and roughness of optical elements. It is important that a method of exact measurement is incorporated in this interferometer to eliminate the undesirable phase distribution.

We review the principle of the SPM Fizeau interferometer using a self-pumped phase-conjugate wave. A laser beam collimated with lenses L1 and L2 is incident on a surface of the object through a beamsplitter BS1. The object field generated by the object surface is written as

$$U_O(x) = \exp[2jkr(x)] \ , \tag{1}$$

where $r(x)$ is the surface profile of the object, x is a coordinate on the object, and k is the wave number. The object wave is bent at right angles by the beamsplitter BS1. Lenses L2 and L3 form an object field in the image space at the surface of the glass plate. The transmitted beam through the glass plate is focused with lens L4 into the self-pumped conjugator of a $BaTiO_3$ crystal, which produces a phase-conjugate wave. The phase-conjugate wave interferes with the object wave on the glass plate. In this interferometer, the phase-conjugate wave is considered as a reference wave, and the beam reflected by the glass plate is considered as the object wave.

Sinusoidal phase modulating interferometry is used to obtain the phase distribution of the interference pattern. To phase-modulate the object beam, the glass plate is sinusoidally vibrated with piezoelectric transducers (PZTs). The vibration of the glass plate is expressed by

$$A(t) = a \cos(\omega_c t + \theta) \ . \tag{2}$$

The reference and object fields on the glass plate can be written as

$$U_{1R}(x') = R \exp[-2jkr(x')] \ , \tag{3}$$

$$U_{1O}(x') = \exp[2jkr(x') + Z \cos(\omega_c t + \theta)] \ , \tag{4}$$

where R is the phase-conjugate reflectivity, $Z = (4\pi/\lambda)a$, and x' is a coordinate on the glass plate. The lens L5 images these fields on a CCD image sensor. The interference pattern generated from $U_{1R}(x')$ and $U_{1O}(x')$ on the CCD image sensor is expressed as

$$I(x'',t) = 1 + R^2 + 2R \cos[Z \cos(\omega_c t + \theta) + \alpha] \ , \tag{5}$$

where

$$\alpha = (8\pi/\lambda)r(x'') \ , \tag{6}$$

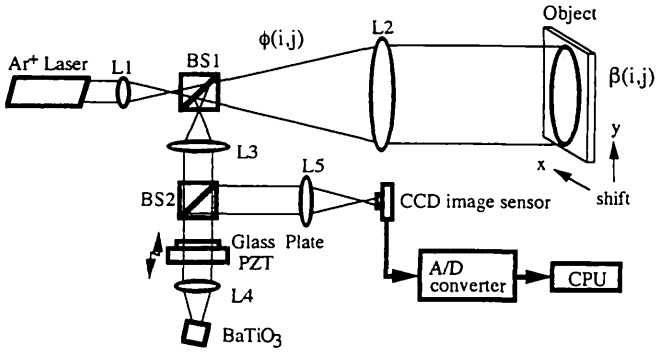

Fig. 1 Exact measurement in a sinusoidal phase-modulating Fizeau interferometer using a self-pumped phase-conjugate wave.

and x'' is a coordinate on the CCD image sensor. The phase α is obtained from the detected signal with the Fourier transform method[8] or the integrating-bucket method.[9]

3 Method of Exact Measurement

When the diameter of an object is large, the diameter of the lens L2 also becomes large and has aberration. Then an undesirable phase distribution ϕ is introduced by the aberrating lens. In this case the phase-conjugate interferometer detects the phase distribution $\alpha = \beta + \phi$, where β is the phase distribution that represents the surface profile of the object. We propose a method for eliminating the undesirable phase distribution to measure exactly the flat surface profile of the object.

First, we detect the phase distribution,

$$\bar{\alpha}(i,j) = \beta(i,j) + \phi(i,j) \ , \quad i = 1 \sim L, \ j = 1 \sim M, \tag{7}$$

where a point (i,j) indicates a measuring point. The measuring points are located at intervals of d_x and d_y in the x-axis and y-axis directions, respectively. We fit the detected raw phase distribution $\bar{\alpha}(i,j)$ to a plane P_α in the least-squares sense across the measuring region of $i = 1 \sim L$ and $j = 1 \sim M$. The mathematical reference plane P_α is expressed as

$$P_\alpha(i,j) = (i - i_c)A_\alpha + (j - j_c)B_\alpha + C_\alpha \ , \quad i = 1 \sim L, \ j = 1 \sim M, \tag{8}$$

where the coordinates (i_c, j_c) are a central point of the measuring region. We obtain the phase distribution $\alpha(i,j)$ by subtracting the tilts A_α and B_α and the average height C_α from the $\bar{\alpha}(i,j)$:

$$\alpha(i,j) = \beta(i,j) + \phi(i,j) - P_\alpha(i,j) \ , \quad i = 1 \sim L, \ j = 1 \sim M. \tag{9}$$

Second, we shift the object in the horizontal direction or the x-axis direction by the interval d_x of the measuring points, as shown in Fig. 1. During this shift, the object surface is generally subjected to an additional displacement besides the shift of d_x. The additional displacement is expressed as

$$D_h(i,j) = (i - i_c)A_h + (j - j_c)B_h + C_h \ , \quad i = 1 \sim L, \ j = 1 \sim M. \tag{10}$$

It is assumed that the undesirable phase distribution ϕ does not change by the shift and the additional displacement of the object surface. This means the object surface is so smooth and the additional displacement is so small that the propagation direction of the light reflected by the object surface almost does not change after the shift of the object. In this condition we detect the phase distribution

$$\bar{\alpha}_h(i,j)=\beta(i+1,j)+\phi(i,j)+D_h(i,j)\ ,$$
$$i=1\sim L,\ j=1\sim M. \tag{11}$$

To eliminate the $D_h(i,j)$, we subtract the tilt and the average height of $\bar{\alpha}_h(i,j)$ from the $\bar{\alpha}_h(i,j)$. We obtain the phase distribution

$$\alpha_h(i,j)=\beta(i+1,j)+\phi(i,j)-P_h(i,j)\ ,$$
$$i=1\sim L,\ j=1\sim M, \tag{12}$$

where the $P_h(i,j)$ is a mathematical reference plane for the phase distribution $\beta(i+1,j)+\phi(i,j)$ across the measuring region of $i=1\sim L$ and $j=1\sim M$. Since the distribution of $\beta(i+1,j)$ across the measuring region is a little different from that of $\beta(i,j)$, the reference plane P_h is a little different from the reference plane P_α.

Third, we shift the object in the vertical direction or the y-axis direction by the interval d_y of the measuring points. In the same way as in the shift of the x-axis direction, we obtain the phase distribution $\alpha_v(i,j)$ by subtracting the tilt and the average height of the raw detected phase distribution $\bar{\alpha}_v(i,j)$ from the $\bar{\alpha}_v(i,j)$:

$$\alpha_v(i,j)=\beta(i,j+1)+\phi(i,j)-P_v(i,j)\ ,$$
$$i=1\sim L,\ j=1\sim M, \tag{13}$$

where the $P_v(i,j)$ is a reference plane for the phase distribution $\beta(i,j+1)+\phi(i,j)$ across the measuring region. The P_v is a little different from the reference plane P_α. The $\alpha_v(i,j)$ also does not contain the additional displacement $D_v(i,j)$ of the object surface, which is caused by the shift of d_y.

Finally, we obtain the following values from the three measured values α, α_h, and α_v as follows:

$$h_d(i,j)=\alpha_h(i,j)-\alpha(i,j)=\beta(i+1,j)-\beta(i,j)+\Delta P_h(i,j)\ ,$$
$$i=1\sim L-1,\ j=1\sim M, \tag{14}$$

$$v_d(i,j)=\alpha_v(i,j)-\alpha(i,j)=\beta(i,j+1)-\beta(i,j)+\Delta P_v(i,j)\ ,$$
$$i=1\sim L,\ j=1\sim M-1, \tag{15}$$

where

$$\Delta P_h(i,j)=P_\alpha(i,j)-P_h(i,j)\ ,$$
$$\Delta P_v(i,j)=P_\alpha(i,j)-P_v(i,j)\ . \tag{16}$$

It is assumed that the differences $\Delta P_h(i,j)$ and $\Delta P_v(i,j)$ are so small that we can neglect them. Under this condition the $h_d(i,j)$ and $v_d(i,j)$ are considered to be equal to the following equations, respectively:

$$h(i,j)=\beta(i+1,j)-\beta(i,j)\ ,\quad i=1\sim L-1,\ j=1\sim M, \tag{17}$$

$$v(i,j)=\beta(i,j+1)-\beta(i,j)\ ,\quad i=1\sim L,\ j=1\sim M-1. \tag{18}$$

These values are the difference values of $\beta(i,j)$ according to i and j, respectively, and they do not contain the undesirable phase distribution ϕ. Effects of the $\Delta P_h(i,j)$ and $\Delta P_v(i,j)$ will be discussed in Sec. 6.

The next step is to calculate the phase β from the h and v, or the difference values of β. For the sake of simplicity, we consider a simple case of 3×3 measuring points, that is, $L=M=3$. The relationship between h, v, and β is given by the matrix representation

$$\begin{bmatrix} h(1,1)\\ h(2,1)\\ h(1,2)\\ h(2,2)\\ h(1,3)\\ h(2,3)\\ v(1,1)\\ v(2,1)\\ v(3,1)\\ v(1,2)\\ v(2,2)\\ v(3,2)\end{bmatrix}=\begin{bmatrix} -1&1&0&0&0&0&0&0&0\\ 0&-1&1&0&0&0&0&0&0\\ 0&0&0&-1&1&0&0&0&0\\ 0&0&0&0&-1&1&0&0&0\\ 0&0&0&0&0&0&-1&1&0\\ 0&0&0&0&0&0&0&-1&1\\ -1&0&0&1&0&0&0&0&0\\ 0&-1&0&0&1&0&0&0&0\\ 0&0&-1&0&0&1&0&0&0\\ 0&0&0&-1&0&0&1&0&0\\ 0&0&0&0&-1&0&0&1&0\\ 0&0&0&0&0&-1&0&0&1\end{bmatrix}\begin{bmatrix}\beta(1,1)\\ \beta(2,1)\\ \beta(3,1)\\ \beta(1,2)\\ \beta(2,2)\\ \beta(3,2)\\ \beta(1,3)\\ \beta(2,3)\\ \beta(3,3)\end{bmatrix} \tag{19}$$

We define a vector $\boldsymbol{\gamma}$ whose elements are $h(i,j)$ and $v(i,j)$ and a vector $\boldsymbol{\beta}$ whose elements are $\beta(i,j)$. Generally, Eq. (19) is reduced to

$$\boldsymbol{\gamma}=A\boldsymbol{\beta}\ . \tag{20}$$

When the measuring points are $L\times M$ points, the vector $\boldsymbol{\beta}$ has LM elements and the vector $\boldsymbol{\gamma}$ has $2LM-(L+M)$ elements. We can solve the linear equation of Eq. (20) for the unknowns $\boldsymbol{\beta}$. We obtain a solution $\boldsymbol{\beta}$ by minimizing the objective function

$$B=\|\boldsymbol{\gamma}-A\boldsymbol{\beta}\|^2 \tag{21}$$

with the conjugate gradient method.[10]

There are different methods to obtain a solution β. We can use a least-squares solution of Eq. (20), or solve Eq. (20) by using a singular value decomposition of the matrix **A**. These matrix computations require a large amount of memory in a computer. If the numbers L and M are 2^n, where n is an integer, we can use fast Fourier transform to obtain a solution β in a short time from the difference equations of Eqs. (17) and (18).[11] As shown above, we adopt the conjugate gradient method that does not require as much memory as the matrix computations and does not impose a restriction on the numbers L and M.

4 Numerical Analysis

We did computer simulations to examine some characteristics of this method. In this simulation we made the difference values of an object $\beta(i,j)$ without considering the D_h, D_v, ΔP_h, and ΔP_v. First, we consider effect of noise contained

in the α, α_h, and α_v. We used Gaussian noise whose mean value and standard deviation σ were zero and 3.1×10^{-2} rad, respectively. The standard deviation 3.1×10^{-2} rad is expressed as $\lambda/200$ in wavelength λ. We made three different noises n_α, n_h, and n_v for the α, α_h, and α_v, respectively. Figure 2(a) shows the noise $n_\alpha(i,j)$, where $L = M = 20$. Standard deviation and peak-valley distance (P-V) of a surface profile of the object $\beta(i,j)$ were 3.1×10^{-1} rad ($\lambda/20$) and 1.5 rad ($\lambda/4$), respectively. The standard deviation of the noise is one-tenth that of the surface profile. We made the distributions of $h(i,j)$ and $v(i,j)$ from the object $\beta(i,j)$ and added the noises of $n_\alpha - n_h$ and $n_\alpha - n_v$ to the h and v, respectively. We obtained an estimated phase distribution of the surface profile $\hat{\beta}(i,j)$ which is shown in Fig. 2(b). The noise $n(i,j)$ contained in the $\hat{\beta}(i,j)$ is shown in Fig. 2(c), and the standard deviation of the noise $n(i,j)$ is 1.2σ. This result indicates that this method provides a good solution $\hat{\beta}(i,j)$ without increasing the noises contained in the detected phase distributions.

Next we consider how much the measurement error occurs when the shifts of the object are not equal to the interval d_x or d_y of the measuring points. The surface profile $\beta(i,j)$ is given at the measuring point (i,j) before the shifts. When the object is shifted by rd_x or rd_y, the value of β on the measuring point (i,j) after the shift is calculated with a linear interpolation from the two adjacent values of β that are close to the point (i,j). We estimated the $\hat{\beta}(i,j)$ from the data calculated in the existence of the shift error and obtained the standard deviation of the difference $\hat{\beta}(i,j) - \beta(i,j)$. The standard deviation of the difference divided by that of $\beta(i,j)$ is referred to as the error E_R. In Fig. 3 the error E_R expressed in percentages is shown as a function of ratio of shift r. Three different cases are considered. In case (1) the horizontal shift in the x direction is rd_x, and the vertical shift in the y direction is d_y. We also have case (2) of d_x and rd_y and case (3) of rd_x and rd_y. The errors in case (1) are larger than those in case (2). This result is due to the fact that the variation of the surface profile $\beta(i,j)$ along the x axis is larger than that along the y axis. If the error E_R is expected to be less than 5%, the ratio of shift must be between 0.92 and 1.08 in case (3). It is not so difficult to get the accuracy of the shift corresponding to these ratios.

5 Exact Measurements of 2-D Surface Profiles

We measured the surface profile of a 40-mm-diam flat mirror in the interferometer shown in Fig. 1. The lens L1 is a 40× microscopic objective lens, and the focal lengths of lenses L2 and L3 were 500 and 70 mm, respectively. The object was placed at 20 mm from lens L2. The distance between L3 and the glass plate was 79 mm to make the object field on the glass plate. The spatial intervals d_x and d_y of the measuring points in the two directions were 0.9 and 1.0 mm, respectively. The flat mirror surface was imaged on the CCD image sensor with a magnification of 0.027. The 40×40 elements of the CCD image sensor were used to detect the interference pattern. The frequency of the sinusoidal phase modulation is 120 Hz. The surface profile was obtained through the integrating-bucket method.

We detect three phase distributions $\bar{\alpha}$, $\bar{\alpha}_h$, and $\bar{\alpha}_v$, and we subtracted the tilts and the average heights, that is, P_α, $P_h + D_h$, and $P_v + D_v$, from them to obtain α, α_h, and α_v, respectively. Figures 4(a), 4(b), and 4(c) show these three

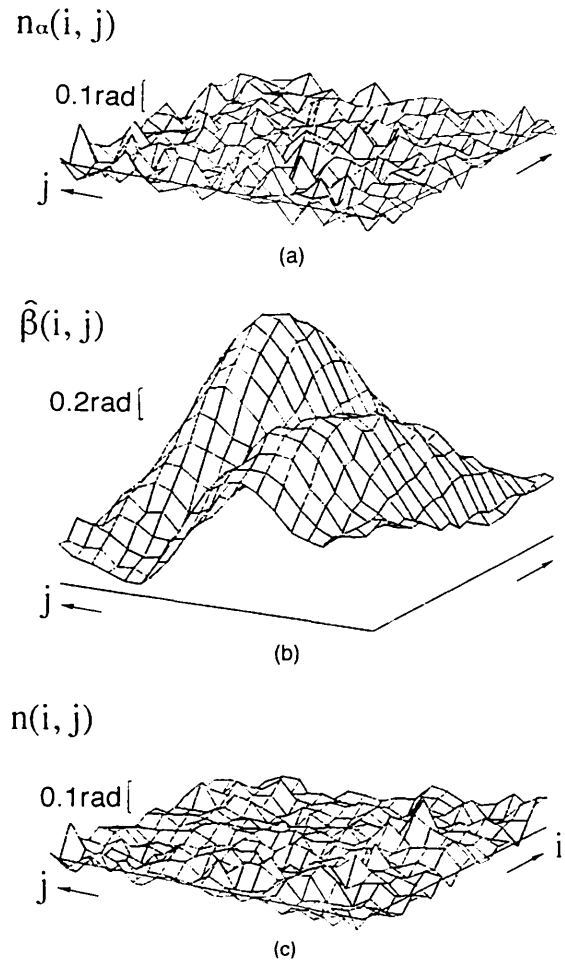

Fig. 2 Effect of noise contained in measured phase distributions: (a) noise $n_\alpha(i,j)$ contained in the phase distribution $\alpha(i,j)$; (b) estimated phase distribution of surface profile $\hat{\beta}(i,j)$; and (c) noise $n(i,j)$ contained in (b).

measured phase distributions α, α_h, and α_v in roughness on a circular region in the 40×40 measuring region. Because these distributions contain the undesirable phase ϕ, the root mean square (RMS) and the P-V of the surface profile are large. The RMS and P-V values are ~115 and ~470 nm, respectively, in these results. The exact surface profile β obtained from the three surface profiles of Figs. 4(a), 4(b), and 4(c) is shown in Fig. 4(d). The RMS and P-V values are 31 and 161 nm, respectively. These results indicate that we can eliminate the undesirable phase and achieve an exact measurement.

6 Discussions

To eliminate the additional displacements D_h and D_v, we define the three different reference planes for the three measurements. Then the difference values of $\beta(i,j)$ contain the ΔP_h and ΔP_v. We examine how much the existence of the ΔP_h and ΔP_v affects the solution of $\beta(i,j)$. We use the experimental results of $\beta(i,j)$ shown in Fig. 4(d) and $\phi(i,j)$ as data of simulations. The distribution of $\phi(i,j)$ is obtained by subtracting the $\beta(i,j)$ from the $\alpha(i,j)$ shown in Fig. 4(a). We made the following distributions for the simulations:

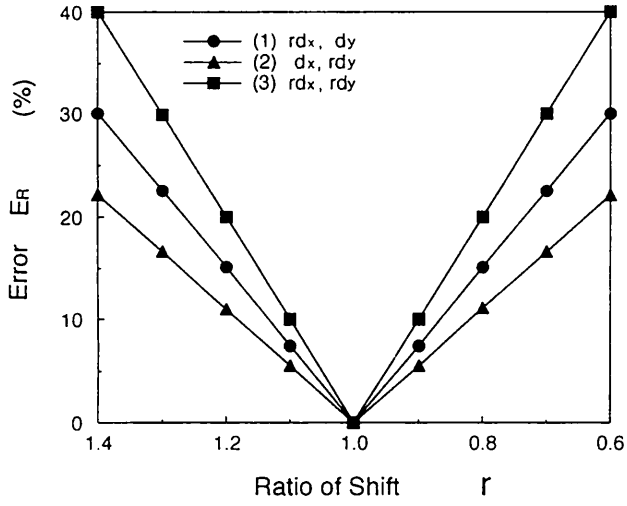

Fig. 3 Effect of error in distance of the shifts on estimated surface profile.

$$\bar{\alpha}(i,j)=\beta(i,j)+\phi(i,j)\ ,$$

$$\bar{\alpha}_h(i,j)=\beta(i+1,j)+\phi(i,j)\ ,$$

$$\bar{\alpha}_v(i,j)=\beta(i,j+1)+\phi(i,j)\ ,\quad i=1\sim 39,\ j=1\sim 39\ . \quad (22)$$

We calculated the reference planes P_α, P_h, and P_v for the distributions $\bar{\alpha}$, $\bar{\alpha}_h$, and $\bar{\alpha}_v$, respectively, and obtained ΔP_h and ΔP_v. The results are shown in Table 1. The A and B are the tilts of a plane for the x-axis and y-axis directions, respectively, and the C is the height of a plane in the direction perpendicular to the x-y plane at the central point (i_c, j_c) of the measuring region. Figure 5 shows the $h(i,j)$ and $v(i,j)$ calculated from the distributions given by Eq. (22). We can see that the values of $\Delta P_h(i,j)$ and $\Delta P_v(i,j)$ are very small compared with the $h(i,j)$ and $v(i,j)$. The P-V value of the $h(i,j)$ is ~55 nm, while the P-V value of the $\Delta P_h(i,j)$ is ~2 nm in the measuring region of ~40 mm as seen from Table 1.

Next, we made the $h_d(i,j)$ and $v_d(i,j)$ by adding the ΔP_h and ΔP_v to the $h(i,j)$ and $v(i,j)$, respectively. We estimated the phase distribution $\hat{\beta}_{39}(i,j)$ in the measuring region of $L=M=39$ from the $h_d(i,j)$ and $v_d(i,j)$ that have the small errors $\Delta P_h(i,j)$ and $\Delta P_v(i,j)$. Figure 6 shows the $\hat{\beta}_{39}(i,j)$ in a circular region, which is almost the same as the $\beta(i,j)$ shown in Fig. 4(d). Figure 7 shows the difference $\hat{\beta}_{39}(i,j)-\beta(i,j)$ whose RMS and P-V values are 20% of those of the $\hat{\beta}_{39}(i,j)$. This result indicates that the measurement error of this method is 20% in RMS and P-V values for the surface profile shown in Fig. 4(d). This error depends on the values of ΔP_h and ΔP_v or the surface profile of the object to be measured.

Finally, we calculated the P_α, P_h+D_h, and P_v+D_v from the raw phase distributions $\bar{\alpha}$, $\bar{\alpha}_h$, and $\bar{\alpha}_v$ detected in the experiments to obtain the values of $\Delta P_h - D_h$ and $\Delta P_v - D_v$. These values are also shown in Table 1. The additional displacements of the object surface involved in the shifts of the object are very large compared with the ΔP_h and ΔP_v. Subtracting the tilt and the average height from the raw detected phase distribution is very effective processing to eliminate the additional displacements, although the processing pro-

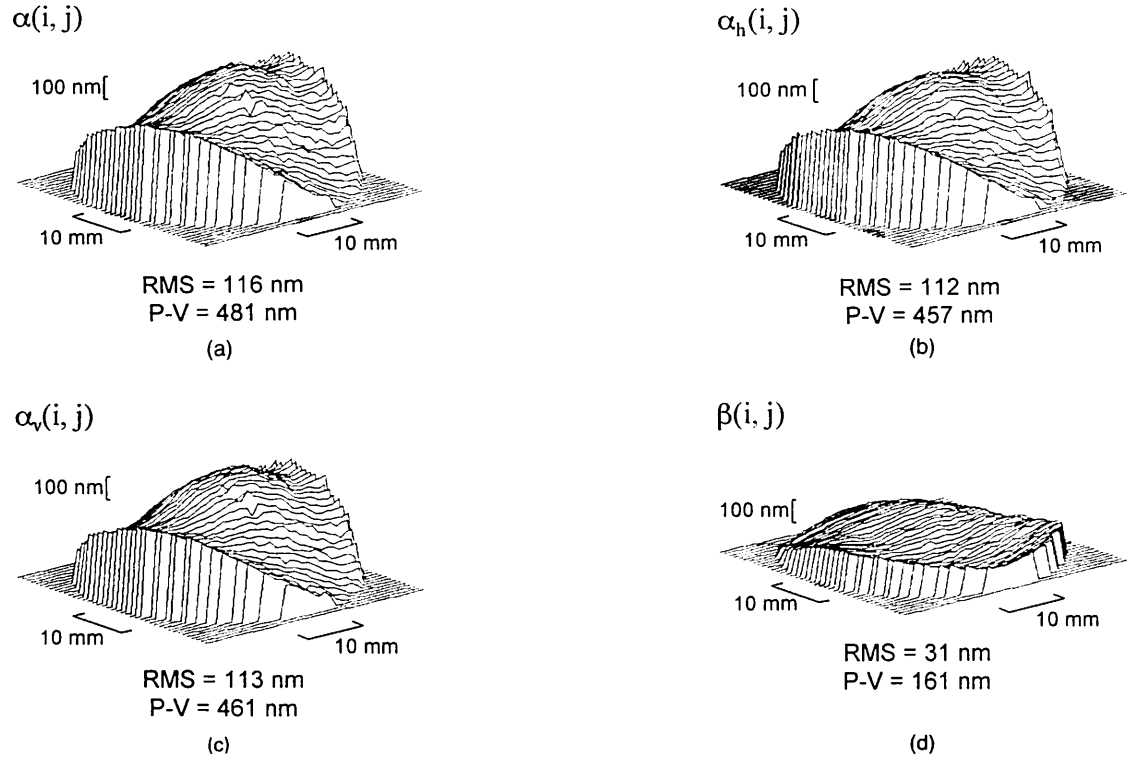

Fig. 4 Experimental results of exact measurement. Phase distributions are expressed as roughness: (a) $\alpha(i,j)$ before the shifts; (b) $\alpha_h(i,j)$ after the shift in the x-axis direction; (c) $\alpha_v(i,j)$ after the shift in the y-axis direction; and (d) estimated surface profile $\beta(i,j)$ of the flat mirror.

Table 1 Values of tilts and average height of planes.

	A (nm/mm)	B (nm/mm)	C (nm)
ΔP_h	-0.03	0.03	0.001
ΔP_v	0.04	0.009	0.05
$\Delta P_h - D_h$	7.6	6.8	13.9
$\Delta P_v - D_v$	-6.1	2.2	-3.9

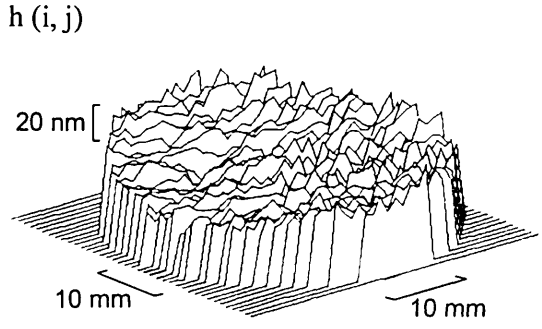

RMS = 8 nm P-V = 55 nm

(a)

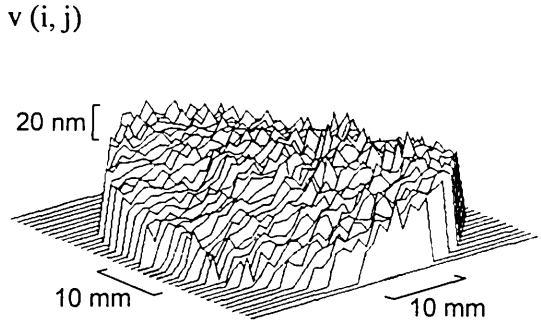

RMS = 9 nm P-V = 52 nm

(b)

Fig. 5 Distributions (a) $h(i,j) = \beta(i+1,j) - \beta(i,j)$ and (b) $v(i,j) = \beta(i,j+1) - \beta(i,j)$, where $i, j = 1 \sim 39$, obtained from the $\beta(i,j)$ shown in Fig. 4(d).

duces the three different reference planes and the existence of the ΔP_h and ΔP_v in the difference values of $\beta(i,j)$. If there are no additional displacements, only the reference plane P_α is defined. Then we can make an absolute measurement.

7 Conclusions

We have proposed a method of exact measurement of flat surface profiles in the phase-conjugate Fizeau interferometer. We tried to measure exactly a surface profile of a 40-mm-diam flat mirror. We shifted the object in the two directions orthogonal to each other by ~1 mm, and we obtained the difference values of the surface profile of the object. Although the additional displacements of the object surfaces involved

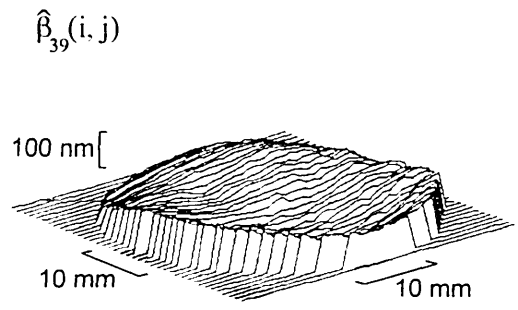

RMS = 26 nm P-V = 128 nm

Fig. 6 Phase distribution $\hat{\beta}_{39}(i,j)$ estimated from the $h_d(i,j)$ and $v_d(i,j)$ that have $\Delta P_h(i,j)$ and $\Delta P_v(i,j)$, respectively.

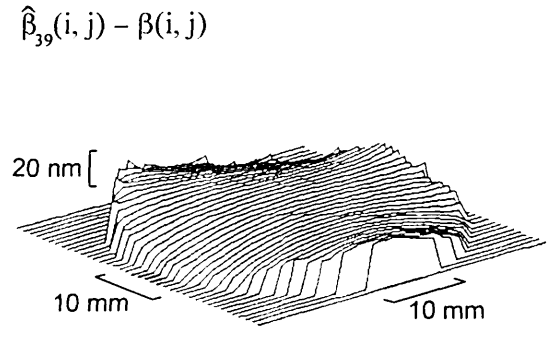

RMS = 4 nm P-V = 28 nm

Fig. 7 Differences of $\hat{\beta}_{39}(i,j) - \beta(i,j)$, where the $\beta(i,j)$ is shown in Fig. 4(d).

in the shifts were very large, the displacements were eliminated by subtracting the tilt and the average height from the raw detected phase distributions. However, this processing defines the three different reference planes for the three measurements and produced the small errors in the difference values of the surface profile. The numerical simulations indicated that the small errors caused the measurement error of 20% in the RMS and P-V values. Exact measurements showed that the RMS and P-V values of the flat mirror were 31 and 161 nm, respectively. On the other hand those values of the flat mirror were ~70 and ~300 nm, respectively, when the undesirable phase distribution caused by aberration of the lenses was not eliminated. The experimental results clearly show that we can measure exactly surface profiles in the phase-conjugate Fizeau interferometer with the method proposed. We will study further in the future about the measurement accuracy that depends on the surface profile of the object.

Acknowledgment

This research started with the opportunity to talk about absolute measurements with Dr. J. E. Greivenkamp when one of the authors, O. Sasaki, was at the Optical Sciences Center, University of Arizona. We are very grateful for his valuable discussions and comments.

References

1. G. Schulz and J. Schiwider, "Interferometric testing of smooth surfaces," in *Progress in Optics*, E. Wolf, Ed., Vol. 13, pp. 93–167, North-Holland, Amsterdam (1976).
2. B. Friz, "Absolute calibration of an optical flat," *Opt. Eng.* **23**(4), 379–383 (1984).
3. G. Schulz and J. Grzanna, "Absolute flatness testing by the rotation method with optimal measuring error compensation," *Appl. Opt.* **31**, 3767–3780 (1992).
4. K. E. Elssner, A. Vogel, J. Grzanna, and G. Schulz, "Establishing a flatness standard," *Appl. Opt.* **33**, 2437–2446 (1994).
5. J. Grzanna and G. Schulz, "Absolute testing of flatness standards at square-grid points," *Opt. Commun.* **77**, 107–112 (1990).
6. J. Grzanna, "Absolute testing of optical flats at points on a square grid: error propagation," *Appl. Opt.* **33**, 6654–6661 (1994).
7. X. Wang, O. Sasaki, Y. Takebayashi, T. Suzuki, and T. Maruyama, "Sinusoidal phase-modulating Fizeau interferometer using a self-pumped phase conjugator for surface profile measurements," *Opt. Eng.* **33**(8), 2670–2674 (1994).
8. O. Sasaki and H. Okazaki, "Sinusoidal phase modulating interferometry for surface profile measurement," *Appl. Opt.* **25**, 3137–3140 (1986).
9. O. Sasaki, H. Okazaki, and M. Sakai, "Sinusoidal phase modulating interferometer using integrating-bucket method," *Appl. Opt.* **26**, 1089–1093 (1987).
10. R. Fletcher and C. M. Reeves, "Function minimization by conjugate gradients," *Computer J.* **7**, 149–154 (1964).
11. K. R. Freischlad and C. L. Koliopoulos, "Modal estimation of a wave front from difference measurements using the discrete Fourier transform," *J. Opt. Soc. Am. A* **3**, 1852–1861 (1986).

Osami Sasaki received the BE and ME degrees in electrical engineering from Niigata University in 1972 and 1974, respectively, and the DrEng degree in electrical engineering from the Tokyo Institute of Technology in 1981. He is a professor of electrical and electronic engineering at Niigata University. Since 1974 he has worked in the field of optical measuring systems and optical information processing.

Yuuichi Takebayashi received the BE degree in electrical engineering from Niigata University in 1993. He has been involved in absolute measurement of surface profiles with interferometers using phase-conjugate waves. He is a graduate student at Niigata University.

Xiangzhao Wang received the BE degree in electrical engineering from Dalian University of Science and Technology, China, in 1982 and the ME degree in electrical engineering from Niigata University in 1992. He is currently working toward a PhD in the Graduate School of Science and Technology at Niigata University. His research interests include optical measuring systems, applications of phase conjugate optics, and optical information processing.

Takamasa Suzuki received the BE degree from Niigata University in 1982, the ME degree from Touhoku University in 1984, and the DrEng degree from the Tokyo Institute of Technology in 1994, all in electrical engineering. He is an associate professor of electrical and electronic engineering at Niigata University. Since 1987 he has worked on interferometers using laser diodes and applications of phase conjugate optics at Niigata University.